

Available online at www.sciencedirect.com**ScienceDirect**

Nuclear Physics B 885 (2014) 448–458

**NUCLEAR
PHYSICS B**www.elsevier.com/locate/nuclphysb

Single-valued Hamiltonian via Legendre–Fenchel transformation and time translation symmetry

Huan-Hang Chi ^{a,b,c}, Hong-Jian He ^{b,c,d}^a *Physics Department, Stanford University, Stanford, CA 94305, USA*^b *Institute of Modern Physics and Center for High Energy Physics, Tsinghua University, Beijing 100084, China*^c *Physics Department, Tsinghua University, Beijing 100084, China*^d *Center for High Energy Physics, Peking University, Beijing 100871, China*

Received 4 May 2014; received in revised form 18 May 2014; accepted 18 May 2014

Available online 23 May 2014

Editor: Stephan Stieberger

Abstract

Under conventional Legendre transformation, systems with a non-convex Lagrangian will result in a multi-valued Hamiltonian as a function of conjugate momentum. This causes problems such as non-unitary time evolution of quantum state and non-determined motion of classical particles, and is physically unacceptable. In this work, we propose a new construction of single-valued Hamiltonian by applying Legendre–Fenchel transformation, which is a mathematically rigorous generalization of conventional Legendre transformation, valid for non-convex Lagrangian systems, but not yet widely known to the physics community. With the new single-valued Hamiltonian, we study spontaneous breaking of time translation symmetry and derive its vacuum state. Applications to theories of cosmology and gravitation are discussed. © 2014 The Authors. Published by Elsevier B.V. This is an open access article under the CC BY license (<http://creativecommons.org/licenses/by/3.0/>). Funded by SCOAP³.

1. Introduction

Conventional physical systems are described by Lagrangians which are convex functions of velocity. Thus, one can derive unique single-valued Hamiltonians by applying the Legendre transformation. This leads to well-defined general formalism of classical and quantum theories.

E-mail addresses: hhchi@stanford.edu (H.-H. Chi), hjhe@tsinghua.edu.cn (H.-J. He).

<http://dx.doi.org/10.1016/j.nuclphysb.2014.05.017>

0550-3213/© 2014 The Authors. Published by Elsevier B.V. This is an open access article under the CC BY license (<http://creativecommons.org/licenses/by/3.0/>). Funded by SCOAP³.

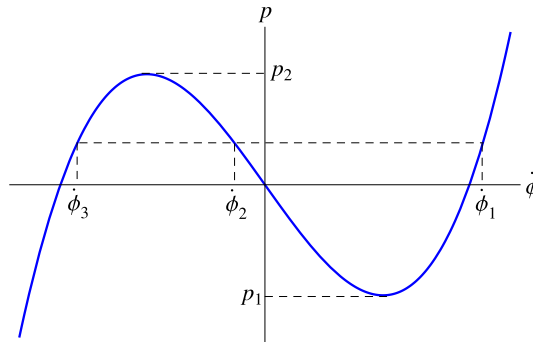


Fig. 1. The Legendre mapping function f from $\dot{\phi}$ to p , for the non-convex Lagrangian (1) with $\kappa > 0$.

Their Lagrangians are quadratic in velocities with positive coefficient, and are thus convex functions. But, physical systems with non-convex Lagrangians are also very interesting, since they are important for studying spontaneous breaking of time translation symmetry [1–3] and are widely applied to theories of cosmology and gravitation [4–9].

Recently, Shapere and Wilczek considered interesting models with non-convex Lagrangians in velocity [1,2]. For the purpose of demonstration, let us consider a simple model [1–3],

$$L = \frac{1}{4}\dot{\phi}^4 - \frac{\kappa}{2}\dot{\phi}^2, \tag{1}$$

to demonstrate the essential idea. For the nontrivial case of $\kappa > 0$, the Lagrangian is a non-convex function of velocity. Thus, the conjugate momentum

$$p = \frac{\partial L}{\partial \dot{\phi}} = \dot{\phi}^3 - \kappa\dot{\phi} \equiv f(\dot{\phi}), \tag{2}$$

is not monotonic in velocity, where the function $f(\dot{\phi})$ stands for the Legendre map. Then, making the conventional Legendre transformation gives the corresponding Hamiltonian as a function of velocity,

$$H = \frac{3}{4}\dot{\phi}^4 - \frac{\kappa}{2}\dot{\phi}^2, \tag{3}$$

which is a multi-valued function (with cusps) in conjugate momentum p , since each given p corresponds to one or three values of $\dot{\phi}$, as shown in Eq. (2).

A multi-valued Hamiltonian will make the evolution of quantum state ill-defined. Since at any moment, for a given ϕ and p , one does not know which “branch” of the multi-valued Hamiltonian could be used to generate the evolution of quantum state. This means that the time evolution of a quantum state may arise from any branch of the naive multivalued Hamiltonian and switch from one branch to another [3], which would cause nonunitary evolution and thus be physically unacceptable [3].

For classical motion, similar reasoning also applies to the Hamiltonian formulation. We can recast this problem by using the Lagrangian (1). The equation of motion from the Lagrangian (1) is given by

$$\frac{d}{dt}p(\dot{\phi}) = 0, \tag{4}$$

which requires

$$p(\dot{\phi}) = \dot{\phi}^3 - \kappa \dot{\phi} \equiv f(\dot{\phi}) = p_0, \quad (5)$$

to be constant in time, where p_0 is given by the initial condition. [Since $\dot{\phi}$ is not continuous and thus non-differentiable with t [3], $\ddot{\phi}$ is not defined. So we will use the integral version (5), instead of (4).] As mentioned earlier, for some p_0 values such as $p_1 < p_0 < p_2$ in Fig. 1,¹ there exist three $\dot{\phi}$ values obeying Eq. (5). Thus, at any moment the propagation of this particle cannot be determined, and since the switching from one $\dot{\phi}$ value to another one could occur instantly, the usual picture of motion is fully lost.

Hence, for systems with a non-convex Lagrangian such as (1), the construction of single-valued Hamiltonian in conjugate momentum space is challenging. Related issues also arise in cosmology models [4–6], in extensions of Einstein gravity involving topological invariants [7,8], and in theories of higher-curvature gravity [9]. To tackle this, a few approaches were proposed in the literature [1,3,10].

As we will show, the real problem with multi-valued Hamiltonian lies in the conventional Legendre transformation (LT) which cannot be naively applied to non-convex Lagrangian (1). In this work, we propose a new construction of single-valued Hamiltonian by using Legendre–Fenchel transformation (LFT). The LFT [11] is a mathematically rigorous and natural generalization of the conventional LT for non-convex and non-analytic functions, although it is not yet widely known to the physics community. Using this new single-valued Hamiltonian, we will study the vacuum state and spontaneous breaking of time translation symmetry. We will further compare the results from different methods, and show that the LFT is the optimal approach to construct the physical Hamiltonian for studying non-convex systems.

2. Legendre–Fenchel transformation and construction of single-valued Hamiltonian

The Hamiltonian is usually derived from Lagrangian via conventional Legendre transformation (LT),

$$H = p\dot{\phi} - L, \quad (6)$$

where $p \equiv \frac{\partial L}{\partial \dot{\phi}}$ is the conjugate momentum. A prerequisite of the Legendre transformation is that the original Lagrangian should be convex and analytic. This is usually taken for granted. But, for non-convex functions [such as (1)] or non-analytic case, the LT collapses and its misuse will cause problems, such as the multi-valuedness of Hamiltonian mentioned above.

To handle the non-convex Lagrangian systems and consistently derive single-valued Hamiltonians, the conventional LT is inappropriate and has to be generalized. Indeed, such a generalized LT is given by the Legendre–Fenchel transformation (LFT) [11], which provides the mathematically rigorous generalization of the conventional LT, valid for non-convex and/or non-analytic Lagrangian systems. For the usual case of convex and analytic functions, the LFT naturally reduces to the LT. The rigorous LFT method is well-established in mathematics [11], but not yet widely known to the physics community. Applying the general LFT method [11], we can rigorously construct the Hamiltonian,

$$H(p) = \sup_{\dot{\phi} \in N(p)} [p\dot{\phi} - L(\dot{\phi})], \quad (7)$$

¹ Note that Eq. (2) or (5) is invariant under $(\phi, p) \rightarrow (-\phi, -p)$. Thus, we have $p_1 = -p_2$ in Fig. 1.

where the symbol \sup stands for supremum in mathematics. In (7), $N(p)$ is defined as

$$N(p) = \{ \dot{\phi} \mid \sup p\dot{\phi} - L(\dot{\phi}) < \infty \}, \tag{8}$$

which is required to ensure the finiteness of Hamiltonian for every given p value.

The LFT construction (7) is also expected from physics intuition. Let us consider the steepest-descent approximation or the principle of least action, which can provide some hints. This requires the Lagrangian $L(\dot{\phi})$ to be minimal, and thus

$$H(s, \dot{\phi}) = s\dot{\phi} - L(\dot{\phi}) \tag{9}$$

becomes *maximal* in $\dot{\phi}$ for every s value, where s is a general quantity independent of $\dot{\phi}$. This requirement is consistent with the LFT (7) after replacing s by the conjugate momentum p .

To make LFT easy to implement, we present its geometric interpretation. Let us consider a function,

$$y(\dot{\phi}) = p(\dot{\phi} - \dot{\phi}_0) + L(\dot{\phi}_0), \tag{10}$$

which stands for a line passing the point $(\dot{\phi}_0, L(\dot{\phi}_0))$ in the $\dot{\phi}$ - y plane, with a slope p . Its intercept is

$$Y(p, \dot{\phi}_0) = -p\dot{\phi}_0 + L(\dot{\phi}_0). \tag{11}$$

Thus, we can rewrite Eq. (7) as

$$\begin{aligned} H(p) &= \sup_{\dot{\phi} \in N(p)} [p\dot{\phi} - L(\dot{\phi})] \\ &= \sup_{\dot{\phi} \in N(p)} -Y(p, \dot{\phi}) = - \inf_{\dot{\phi} \in N(p)} Y(p, \dot{\phi}), \end{aligned} \tag{12}$$

where the symbol \inf stands for infimum in mathematics. Hence, the Hamiltonian $H(p)$ obtained from LFT just equals the minimal intercept (with an overall sign flip) of a line with slope p and crossing the curve $L(\dot{\phi})$ in the $\dot{\phi}$ - y plane. This approach is also called the supporting line method [11].

With this geometric interpretation, we are ready to explicitly construct the single-valued Hamiltonian via LFT. For simplicity, we set $\kappa = 1$ from now on. This will not affect essential features of the analysis and restoring a general parameter $\kappa > 0$ is straightforward. Now, the values of p_1 and p_2 shown in Fig. 1 are fixed as

$$p_1 = -\frac{2}{3\sqrt{3}}, \quad p_2 = \frac{2}{3\sqrt{3}}. \tag{13}$$

Note that the Lagrangian (1) is analytic. So the minimal intercept is reached when the line (10) is tangent to the Lagrangian curve. There may be several tangent points for a given slope p , and we should choose the one which minimizes the intercept. For $p \in (\frac{2}{3\sqrt{3}}, +\infty)$, we find from Fig. 1 that the tangent point to the Lagrangian curve is unique,

$$\dot{\phi}_1(p) = \frac{(\frac{2}{3})^{\frac{1}{3}}}{(9p + \sqrt{3}\sqrt{-4 + 27p^2})^{\frac{1}{3}}} + \frac{(9p + \sqrt{3}\sqrt{-4 + 27p^2})^{\frac{1}{3}}}{2^{\frac{1}{3}}3^{\frac{2}{3}}}. \tag{14}$$

Similar reasoning applies for $p \in (-\infty, -\frac{2}{3\sqrt{3}})$, and the corresponding tangent point is

$$\dot{\phi}_3(p) = -\frac{1 + \sqrt{3}i}{2^{\frac{2}{3}}3^{\frac{1}{3}}(9p + \sqrt{3}\sqrt{-4 + 27p^2})^{\frac{1}{3}}} - \frac{(1 - \sqrt{3}i)(9p + \sqrt{3}\sqrt{-4 + 27p^2})^{\frac{1}{3}}}{2^{\frac{4}{3}}3^{\frac{2}{3}}}. \tag{15}$$

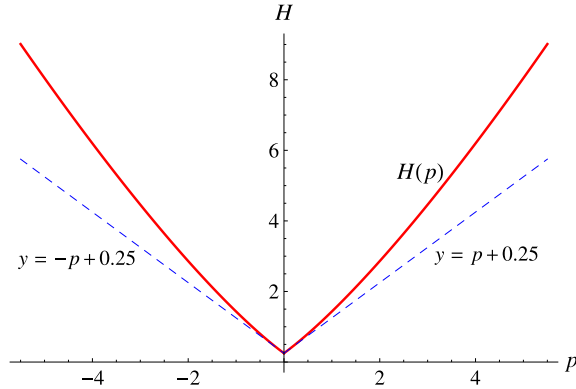


Fig. 2. Hamiltonian H obtained via Legendre–Fenchel transform (LFT) as a function of conjugate momentum p . For comparison, we have also added two extra blue straight dashed-lines $y = \pm p + 0.25$ as reference to make it clear that our Hamiltonian is not a glue of two straight lines. (For interpretation of the references to color in this figure legend, the reader is referred to the web version of this article.)

We note that although i appears in (15), the right-hand side of (15) is actually real-valued for $p \in (-\infty, -\frac{2}{3\sqrt{3}})$.

Then, let us consider the interesting range, $p \in [-\frac{2}{3\sqrt{3}}, \frac{2}{3\sqrt{3}}]$. In this case, there are three tangent points with velocities $(\dot{\phi}_3, \dot{\phi}_2, \dot{\phi}_1)$, whose values are shown in Fig. 1. To minimize the intercept, we find that for $p \in [0, \frac{2}{3\sqrt{3}}]$ the right tangent point as shown in (14) gives the minimum; while for $p \in [-\frac{2}{3\sqrt{3}}, 0)$ the left tangent point as shown in (15) is our choice. And for $p = 0$, the right and left tangent points give the same minimal intercept. These functions are all real-valued in their defined ranges, and everything is consistent. With these, we deduce the Hamiltonian from LFT,

$$\begin{aligned} H(p) &= p\dot{\phi}_1(p) - L(\dot{\phi}_1(p)), \quad \text{for } p \in [0, +\infty), \\ H(p) &= p\dot{\phi}_3(p) - L(\dot{\phi}_3(p)), \quad \text{for } p \in (-\infty, 0), \end{aligned} \tag{16}$$

where $\dot{\phi}_1(p)$ and $\dot{\phi}_3(p)$ are defined in Eqs. (14)–(15). This Hamiltonian is shown in Fig. 2, where we have added two extra straight dashed-lines for reference to make it clear that our Hamiltonian is not a combination of two straight lines as it might appear. Since we have,

$$H(0) = 0.25, \quad \lim_{p \rightarrow 0^\pm} H'(p) = \pm 1, \tag{17}$$

these two dashed-lines are defined as, $H = \pm p \pm 0.25$.

3. Spontaneous breaking of time translation symmetry and comparisons

After constructing the single-valued Hamiltonian via LFT, we are ready to study its physical application and compare it with other approaches in the literature, such as the Hamiltonian path-integral (HPI) method [3] and the naive multi-valued Hamiltonian (3). We will show that our Hamiltonian (16) gives the optimal description of systems with non-convex Lagrangians such as (1).

In Fig. 3, we present the Hamiltonians derived by the LFT approach (Curve-A), the HPI method (Curve-B), and the multi-valued Hamiltonian method (Curve-C). In particular, Curve-A

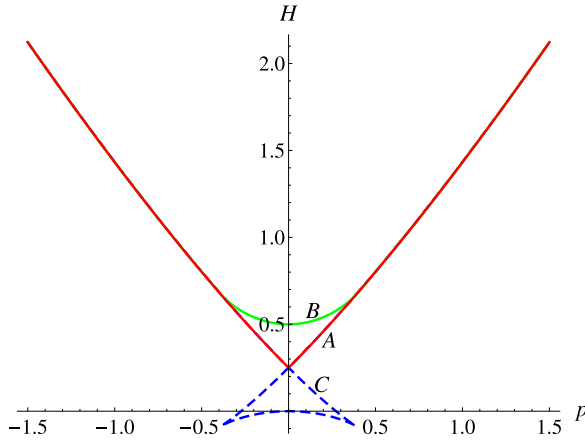


Fig. 3. Comparison of different Hamiltonians: Curve-A (red) and Curve-B (green) are obtained via our LFT approach and HPI method [3], respectively; Curve-C is the multi-valued Hamiltonian which overlaps with Curve-A and has an extra “swallow tail” (blue dashed). These three curves coincide over wide ranges except the central domain around $p = 0$. (For interpretation of the references to color in this figure legend, the reader is referred to the web version of this article.)

is given by the new Hamiltonian (16), and Curve-C is from the multi-valued Hamiltonian (3). We see that the Hamiltonians of our LFT approach (Curve-A) and the HPI method (Curve-B) are both single-valued. Furthermore, Curve-A predicts a ground state of lower energy than that of Curve-B.

Then, we analyze the corresponding Lagrangians by the three methods. For the LFT approach, we deduce the revised Lagrangian from the single-valued Hamiltonian (16),

$$\begin{aligned}
 L_{\text{LFT}}(\dot{\psi}) &= \frac{1}{4}\dot{\psi}^4 - \frac{1}{2}\dot{\psi}^2, \quad \text{for } \dot{\psi} \in (-\infty, -1) \cup (1, +\infty), \\
 L_{\text{LFT}}(\dot{\psi}) &= -\frac{1}{4}, \quad \text{for } \dot{\psi} \in [-1, 1],
 \end{aligned}
 \tag{18}$$

where ψ is the coordinate of the configuration space inferred from the Hamiltonian (16), and needs not to match the previous ϕ . Eq. (18) differs from the original Lagrangian (1) in the range $\dot{\psi} \in [-1, 1]$. It also differs from the Lagrangian obtained by the HPI method [3].

We present the comparison in Fig. 4. It is apparent that the Lagrangian (18) is the convex hull of the original Lagrangian (1), i.e., the largest convex function satisfying $L_{\text{LFT}}(\dot{\phi}) \leq L(\dot{\phi})$. This is expected. We note that the revised Lagrangian (18) may be viewed as the “kinetic version” of Maxwell construction for thermodynamic free energy [12], which means that the state expressed as the red straight-line part of Fig. 4 is a mixture of $\dot{\phi} = -1$ and $\dot{\phi} = +1$ states, similar to the mixing state of water and vapor during evaporation. This also leads to Eq. (23).

Now, we are ready to discuss the vacuum state and the spontaneous breaking of the time translation symmetry. Using the multi-valued Hamiltonian, the analysis in [2] shows that the vacuum state obtained at the cusp of the Hamiltonian gives,

$$H_0 = -\frac{1}{12}, \quad p_0 = \pm \frac{2}{3\sqrt{3}}, \quad \dot{\phi}_0 = \mp \sqrt{\frac{1}{3}},
 \tag{19}$$

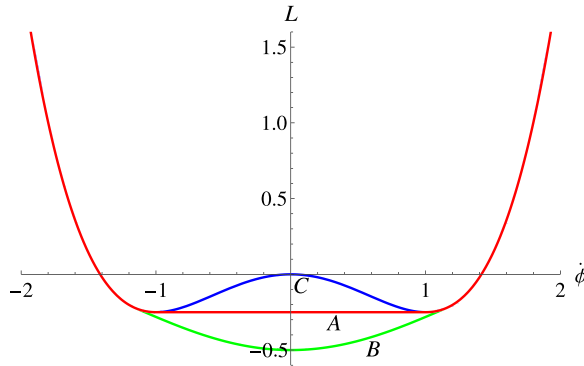


Fig. 4. Comparison of different Lagrangians: Curve-A and -B are Lagrangians inferred from the present LFT Hamiltonian (16) and the HPI Hamiltonian [3], respectively; Curve-C is the original Lagrangian (1).

leading to spontaneously broken time translation invariance. Next, for the HPI method [3], one can infer the vacuum state from Fig. 3,

$$H_0 = \frac{1}{2}, \quad p_0 = 0. \tag{20}$$

Since the HPI does not provide a clear relation between $\dot{\phi}$ and p , we may use the canonical equation of the Hamiltonian given by HPI to obtain the velocity of vacuum state,

$$\dot{\psi}_0 = \left. \frac{\partial H(p)}{\partial p} \right|_{p=0} = 0, \tag{21}$$

where ψ is the coordinate of the configuration space inferred from the Hamiltonian via usual LT. Thus, the time translation symmetry is unbroken in the HPI formalism.

Finally, for the LFT approach, we can deduce the vacuum state from Fig. 2 and Eqs. (14)–(15),

$$H_0 = \frac{1}{4}, \quad p_0 = 0, \quad \dot{\phi}_0 = \pm 1. \tag{22}$$

In this case, the time translation symmetry is also spontaneously broken.

We also note that it is better to take the original Lagrangian (1) only as a starting point because it is non-convex and thus ill-defined, as commented in [3]. After obtaining a physical Hamiltonian, we can rederive a revised physical Lagrangian, together with a revised coordinate ψ of the configuration space, via the LFT. So, let us derive this coordinate ψ from the Hamiltonian (16), which needs not to match the previous ϕ . Then, inspecting the vacuum state of Curve-A in Fig. 3, we deduce

$$\dot{\psi}_0 \in [-1, 1], \tag{23}$$

i.e., the velocity of vacuum state could pick up any value in the range $[-1, 1]$. Eq. (23) should precisely describe the vacuum state. We note that the values of $\dot{\psi}_0 \in [-1, 1]$ always spontaneously break the time translation symmetry, except a single point at $\dot{\psi}_0 = 0$ which however only has zero measure over the full interval $[-1, 1]$.

4. Conclusions and discussions

The recent inspiring works of Shapere and Wilczek [1,2] opened up renewed interests in studying systems with non-convex Lagrangians and spontaneous breaking of time translation

symmetry, as well as applications to cosmology and gravitation [4–9]. In this work, we proposed a new construction of single-valued Hamiltonian by applying Legendre–Fenchel transformation (LFT) [11], which rigorously generalize the conventional Legendre transformation for non-convex and non-analytic functions. We show that this provides a consistent and optimal formulation in which the corresponding revised Lagrangian is the convex hull of the original Lagrangian. Then, we studied the vacuum state and the spontaneous breaking of time translation symmetry, as shown in Fig. 2. We further compared our predictions with those from other methods in the literature. The results inferred from different methods are distinctive with each other (Fig. 3), and can be discriminated by experiments. In Fig. 4, we compared our revised Lagrangian (18) with those from other methods. Using the new coordinate of configuration space ψ , we inferred the degenerate vacuum states with (23).

Finally, it is interesting to further apply our new LFT approach to related systems, such as specific models of cosmology and gravitation [4–9]. For instance, Refs. [5,6] proposed the ghost inflation scenario where an inflationary de Sitter phase is achieved with a ghost condensate. It consistently modifies gravity in the infrared, and is realized via a derivatively coupled ghost scalar field ϕ which forms condensates with non-zero velocity in the background, $\langle \dot{\phi} \rangle = M^2 \neq 0$. This is a new kind of physical fluid filling the universe and has fluctuation $\hat{\phi}$ defined as, $\phi = M^2 t + \hat{\phi}$. This scenario gives an alternative realization of the de Sitter phase, and the scalar ϕ can naturally serve as inflaton [6]. The nonzero ghost condensate $\langle \dot{\phi} \rangle \neq 0$ also spontaneously breaks time translation symmetry, which is just the physical picture quantitatively demonstrated in the present work by applying our new LFT method. Indeed, the LFT method provides a rigorous and consistent way to analyze such cosmological systems. As another example, the recent work (in the first paper of Ref. [9]) studied phase transitions of higher-curvature gravity theories. Similar to our Eq. (1), it considered an extended non-convex Lagrangian, $L = \frac{1}{2}\dot{\phi}^2 - \frac{1}{3}\phi^3 + \frac{1}{17}\dot{\phi}^4$, by applying the LFT method to derive its convex hull (similar to the Curve-A of our Fig. 4). The Lovelock gravity was taken as an explicit model for the analysis [9]. More applications of our LFT method to such gravity and cosmology models will be pursued further.

Acknowledgements

We thank Nima Arkani-Hamed for useful discussions. This work was supported by National Natural Science Foundation of China (under grants 11275101, 11135003) and National Basic Research Program (under grant 2010CB833000).

Appendix A. Derivations of Eq. (18) and Eq. (23)

In this appendix, we present the detailed derivations of Eq. (18) and Eq. (23) from Eq. (16) under the LFT. Similar to Eq. (7), we have

$$L_{\text{LFT}}(\dot{\psi}) = \sup_{p \in M(\dot{\psi})} [p\dot{\psi} - H(p)], \tag{24}$$

where

$$M(\dot{\psi}) = \{ p \mid \sup p\dot{\psi} - H(p) < \infty \} \tag{25}$$

guarantees the finiteness of the Lagrangian for every given $\dot{\psi}$. Following the geometric explanation in Section 2, Eq. (24) can also be regarded as the minimal intercept (with an overall sign flip) of a straight line with slope $\dot{\psi}$ and crossing the curve $H(p)$ in the (p, L_{LFT}) plane. Thus, from

Fig. 2 and for $\dot{\psi} \in (1, \infty)$, we obtain the minimal intercept when the line is tangent to $H(p)$, and the relation between $\dot{\psi}$ and p is, $p = \dot{\psi}^3 - \dot{\psi} \in (0, \infty)$, derived from $\dot{\psi} = \partial H / \partial p$ in this domain. The same reasoning applies for $\dot{\psi} \in (-\infty, -1)$. So, we deduce,

$$\begin{aligned} p &= \dot{\psi}^3 - \dot{\psi} \in (0, \infty), & \text{for } \dot{\psi} \in (1, \infty), \\ p &= \dot{\psi}^3 - \dot{\psi} \in (-\infty, 0), & \text{for } \dot{\psi} \in (-\infty, -1). \end{aligned} \quad (26)$$

For the region $\dot{\psi} \in [-1, 1]$, we reach the minimal intercept when the line crosses the curve $H(p)$ at point $(0, H(0))$. Thus, we have

$$p = 0, \quad \text{for } \dot{\psi} \in [-1, 1], \quad (27)$$

which just coincides Eq. (23). Hence, unlike the previous relation (2), our Eqs. (26)–(27) give the conjugate-momentum p as a monotonic function of velocity $\dot{\psi}$. With the above, we can derive the new Lagrangian from Eq. (24),

$$\begin{aligned} L_{\text{LFT}}(\dot{\psi}) &= \frac{1}{4}\dot{\psi}^4 - \frac{1}{2}\dot{\psi}^2, & \text{for } \dot{\psi} \in (-\infty, -1) \cup (1, \infty). \\ L_{\text{LFT}}(\dot{\psi}) &= -H(0) = -\frac{1}{4}, & \text{for } \dot{\psi} \in [-1, 1]. \end{aligned} \quad (28)$$

This just reproduces our Eq. (18).

Appendix B. Discussing the previous approaches

In this Appendix, for completeness we discuss the previous different attempts in the literature [1,3] for tackling the multi-valued Hamiltonian, which are independent of our current study. Ref. [3] adopted a Hamiltonian path-integral (HPI) method, defined in the position-velocity space, where the transition amplitude $\langle \phi_2, t_2 | \phi_1, t_1 \rangle$ is given by

$$\iint \mathcal{D}\phi(t) \mathcal{D}u(t) \prod_t \frac{\partial^2 L}{\partial u \partial u} \exp \left\{ \frac{i}{\hbar} S_H[\phi(t), u(t)] \right\}. \quad (29)$$

Then, the authors tried to sum up all paths in (ϕ, u) which correspond to the same path in phase-space (ϕ, p) . This would result in an effective Hamiltonian H_{eff} as a single-valued function of conjugate-momentum p . Note that the Hamiltonian H is conventionally defined in the canonical space (ϕ, p) via usual Legendre transformation (LT), which is multi-valued function of velocity u (or, $\dot{\phi}$) for each given $p \in (p_1, p_2)$. So, given such an ill-defined Hamiltonian, it is fully unknown *a priori* which solutions of $\dot{\phi}$ or which paths in (ϕ, u) space are physically (un)acceptable. As shown in Section 2, because the conventional LT is ill-defined for non-convex Lagrangian (1), it is likely that some or all of the $\dot{\phi}$ solutions are nonphysical. Hence, the naive sum of all paths in (ϕ, u) [3] may not be physically meaningful, although one could take it as a working ansatz [3].

The recent approach [1] proposed a new method of branched quantization, which unfolds the non-monotonic $p(\dot{\phi})$ by redefining the conjugate momentum as,

$$\begin{aligned} \xi &\equiv p - p_2 + p_1, & \text{for } \xi \leq p_1, \\ \xi &\equiv -p + p_2 + p_1, & \text{for } p_1 \leq \xi \leq p_2, \\ \xi &\equiv p + p_2 - p_1, & \text{for } p_2 \leq \xi. \end{aligned} \quad (30)$$

We can reexpress (30) as follows,

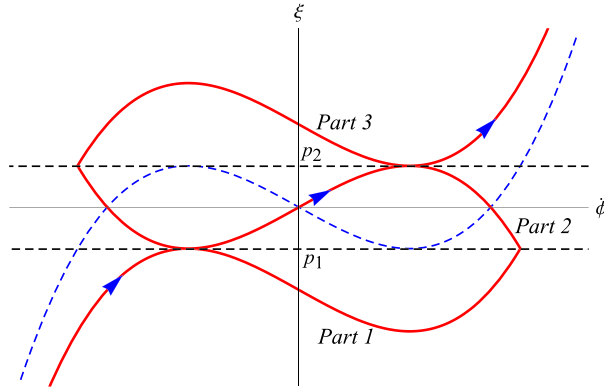


Fig. 5. The relation between $\dot{\phi}$ and ξ , inferred from Eq. (30) or (31). Part-1, -2 and -3 of the red solid curve is obtained by the first, second and third branch of Eq. (30) or (31), respectively. The blue dashed curve $p(\dot{\phi})$ is re-plotted from Fig. 1 as a reference, with the vertical axis labeled by p . (For interpretation of the references to color in this figure legend, the reader is referred to the web version of this article.)

$$\begin{aligned} \xi &\equiv p - p_2 + p_1, & \text{for } p \leq p_2, \\ \xi &\equiv -p + p_2 + p_1, & \text{for } p_1 \leq p \leq p_2, \\ \xi &\equiv p + p_2 - p_1, & \text{for } p_1 \leq p. \end{aligned} \tag{31}$$

As clearly shown, the ranges of p in the three branches overlap with each other in (31). So, each given p corresponds to three ξ values over the range of $p_2 > p > p_1 = -p_2$. As such, the Hamiltonian is still a multi-valued function of new conjugate momentum ξ , because it is easy to verify from (2) or (5) that the equation $\dot{\phi}^3 - \kappa\dot{\phi} = p = -\xi$ still has three solutions $\dot{\phi}$ for each given $\xi \in (p_1, p_2)$ in (30).

To be intuitive, we further explicitly present Eq. (30) or Eq. (31) in Fig. 5 as denoted by the red solid curve. Part-1, -2, and -3 of the red curve are obtained by the first, second, and third branch of Eq. (30) or (31), respectively. For reference, we also plot the blue dashed curve $p(\dot{\phi})$ (from Fig. 1) with the vertical axis labeled by p . From the red curve in Fig. 5, it is apparent that ξ is not a simple function of $\dot{\phi}$. There are three routes which form two extra loops; and only the middle one (marked by arrows) is what Ref. [1] hoped to realize. But, the other two routes are also contained in Eq. (30) or (31). Thus, Eqs. (30)–(31) appear ill-defined and the problem of multi-valued Hamiltonian remains unsolved. If we really want to pick up one route out of the three options, say, the middle one as implied in Ref. [1], we have to add further restrictions to realize it, such as by imposing the supremum condition in the LFT (7). Since the LFT is both physically well-motivated and mathematically rigorous, it is the optimal approach to handle such singular systems.

In addition, Ref. [1] tried to impose certain boundary conditions for ensuring the unitary evolution for multivalued Hamiltonian. As we explicitly clarify in the following, unfortunately this does not work. Ref. [1] defined three branches of wave functions in the paragraph below its Eq. (3), i.e., $\psi_1(p)$ for $-\infty < p \leq p_+$, $\psi_2(p)$ for $p_- \leq p \leq p_+$, and $\psi_3(p)$ for $p_- \leq p < \infty$. It is clear that all three components cover the range $p_- \leq p \leq p_+$, as stated at the end of the same paragraph [1]. Hence, for the boundary conditions (6) of Ref. [1] to ensure the vanishing probability current $j = 0$ at the two junctions $p = p_{\pm}$, all the three branches of wave functions $\psi_{1,2,3}(p)$ [rather than just two branches $\psi_{1,2}(p)$] will contribute to j , so they have to be included

together. This means that Eq. (6) of Ref. [1] with $\psi_{1,2}(p)$ alone cannot actually ensure $j = 0$ at $p = p_+$, and thus the integrated probability $\int \rho$ is not conserved (contrary to the claim of Ref. [1]); the same flaw exists for $p = p_-$. Furthermore, because of the $\psi_3(p)$ contributions to the boundary conditions at $p = p_{\pm}$, Eq. (6) (at $p = p_+$) and its analogues (at $p = p_-$) will contain *extra* 4 ($= 2 + 2$) constraints, so there are actually $4 + 4 = 8$ constraints at $p = p_{\pm}$. Together with the two normalizability conditions at $p \rightarrow \pm\infty$ [1], the total number of boundary constraints is 10, which does not match the number of integral constants $n = 2 \times 3 = 6$ of the Schrödinger equations for $\psi_{1,2,3}(p)$. Unfortunately, these complete boundary conditions over-constrain the system, so this boundary condition method [1] does not really work. (The similar problems also exist for related applications in Ref. [13].)

References

- [1] Alfred Shapere, Frank Wilczek, Phys. Rev. Lett. 109 (2012) 200402, arXiv:1207.2677 [quant-ph].
- [2] Alfred Shapere, Frank Wilczek, Phys. Rev. Lett. 109 (2012) 160402, arXiv:1202.2537 [cond-mat].
- [3] M. Henneaux, C. Teitelboim, J. Zanelli, Phys. Rev. A 36 (1987) 4417.
- [4] C. Armendariz-Picon, T. Damour, V.F. Mukhanov, Phys. Lett. B 458 (1999) 209, arXiv:hep-th/9904075.
- [5] N. Arkani-Hamed, H.C. Cheng, M. Luty, S. Mukohyama, J. High Energy Phys. 0405 (2004) 074, arXiv:hep-th/0312099.
- [6] N. Arkani-Hamed, P. Creminelli, S. Mukohyama, M. Zaldarriaga, J. Cosmol. Astropart. Phys. 0404 (2004) 001, arXiv:hep-th/0312100.
- [7] C. Teitelboim, J. Zanelli, Class. Quantum Gravity 4 (1987) L125.
- [8] C. Teitelboim, J. Zanelli, in: C. Longhi, L. Lusanna (Eds.), Constraints Theory and Relativistic Dynamics, World Scientific, 1987.
- [9] For the latest developments, X.O. Camanho, J.D. Edelstein, G. Giribet, A. Gomberoff, arXiv:1311.6768 [hep-th]; E. Avraham, R. Brustein, arXiv:1401.4921 [hep-th], and references therein.
- [10] L. Zhao, P. Yu, W. Xu, Mod. Phys. Lett. A 28 (2013) 1350002, arXiv:1206.2983 [hep-th].
- [11] For a comprehensive monograph, see R.T. Rockafellar, Convex Analysis, Princeton University Press, Princeton, 1970.
- [12] E.g., M.E. Peskin, D.V. Schroeder, An Introduction to Quantum Field Theory, Westview Press, 1995, pp. 368–369.
- [13] A.D. Shapere, F. Wilczek, Z. Xiong, arXiv:1210.3545 [hep-th].